1 **Part-load Performance of Direct-firing and Co-firing of Coal and Biomass in a Power**

2 **Generation System Integrated with a CO₂ Capture and Compression System**

3 Usman Ali[a, c,*], Muhammad Akram[a], Carolina Font-Palma[b], Derek B Ingham[a], Mohamed

4 Pourkashanian[a]

5 [a]*Energy 2050, Energy Engineering Group, Faculty of Engineering, University of Sheffield, Faculty of*

6 *Engineering, S10 2TN, UK*

7 [b]*Department of Chemical Engineering, Thornton Science Park, University of Chester, CH2 4NU, UK*

8 [c]*Department of Chemical Engineering, University of Engineering and Technology, Lahore – 54890, Pakistan*

9 **Abstract:**

10 Bioenergy with Carbon Capture and Storage (BECCS) is recognised as a key technology to

11 mitigate CO_2 emissions and achieve stringent climate targets due to its potential for negative

12 emissions. However, the cost for its deployment is expected to be higher than for fossil-based

13 power plants with CCS. To help in the transition to fully replace fossil fuels, co-firing of coal

14 and biomass provide a less expensive means. Therefore, this work examines the co-firing at

15 various levels in a pulverised supercritical power plant with post-combustion CO_2 capture,

16 using a fully integrated model developed in Aspen Plus. Co-firing offers flexibility in terms of

17 the biomass resources needed. This work also investigates flexibility within operation. As a

18 result, the performance of the power plant at various part-loads (40%, 60% and 80%) is studied

19 and compared to the baseline at 100%, using a constant fuel flowrate. It was found that the net

20 power output and net efficiency decrease when the biomass fraction increases for constant heat

21 input and constant fuel flow rate cases. At constant heat input, more fuel is required as the

22 biomass fraction is increased; whilst at constant fuel input, derating occurs, e.g. 30% derating

---

* Corresponding Author: chemaliusman@gmail.com

23 of the power output capacity at firing 100% biomass compared to 100% coal. Co-firing of coal

24 and biomass resulted in substantial power derating at each part-load operation.

25 *Key words*: Co-firing; post-combustion; part-load; CO_2 compression; BECCS

26

27 **1. Introduction**

28 Biomass is becoming increasingly more important for achieving EU emission reduction targets

29 as a renewable energy source (Bertrand et al., 2014). In the UK, bioenergy is mostly used to

30 provide heat or power, where 5.2 GW of bio-power and 3.1 GW of heat were produced at the

31 end of July 2016 (BEIS, 2016). A recent report on trends and projections towards Europe's

32 climate and energy targets for 2020 has shown that in 2013 the European greenhouse gas

33 (GHG) emissions were 19 % lower than the 1990 levels and expected to be 24 % lower by

34 2020 (Barbu et al., 2014). However, a later report suggested that the pace of GHG reductions

35 will slow down, and by 2030 the EU emissions reduction will be 27-30 % lower than the 1990

36 levels rather than the target value of 40 % (Barbu et al., 2015). In order to meet the target, there

37 may be an increase in the use of biomass for heat and power to increase the renewable's share

38 of the total energy produced. It is predicted that biomass exploitation capacity in the EU will

39 increase to 1.5-1.8 billion tons in 2030 (EU Commission, 2006).

40 Biomass in combination with coal, termed as co-firing, represents one possible option for

41 reducing CO_2 emissions (Heller et al., 2004; Jia et al., 2016; Mann and Spath, 2001; Ortiz et

42 al., 2011; Rigamonti et al., 2012; Sebastián et al., 2011) and can add flexibility to the system.

43 In addition to reducing GHG emissions, co-firing has added advantages. Co-firing can result

44 in the reduction of NO_x and SO_x emissions, depending upon the type of fuel and operational

45 conditions (De and Assadi, 2009). Furthermore, co-firing can result in the reduction in

46 corrosion, fouling and slagging problems caused by firing biomass alone (Davidsson et al.,

47 2008; NETBIOCOF, 2016; Tillman, 2000). However, a drop-in efficiency of the boiler can be

48 expected due to co-firing which is modest at lower co-firing ratios (De and Assadi, 2009;

49 Hughes and Tillman, 1998; NETBIOCOF, 2016).

50 During co-firing, biomass and coal result in synergistic interaction due to the presence of

51 volatiles in biomass (Oladejo et al., 2017; Sung et al., 2016; Tilghman and Mitchell, 2015).

52 There is a dominant synergistic impact of co-firing woody biomass with coal under air staged

53 conditions on the emissions of NO_x due to lower carbon content but higher volatile matter in

54 biomass (Sung et al., 2016). Tilghman and Mitchell, (2015) developed an intrinsic chemical

55 reactivity model to predict char conversion rates by using the mass lost data during combustion

56 and gasification. The heterogeneous reaction mechanism model is used to accurately predict

57 the effects of heterogeneous reactions in combustion, gasification and oxy-fuel environments

58 (Tilghman and Mitchell, 2015). Oladejo et al. (2017) developed an index to quantify the degree

59 of synergistic interactions which can be used to select the proper biomass and blending ratio at

60 co-fired power plants.

61 Co-firing biomass has also been found to be beneficial during the gasification process. During

62 steam co-gasification of 50:50 wt. % coal:switchgrass mixtures in a pilot-scale bubbling

63 fluidized bed, Masnadi et al. (2015c) observed higher hydrogen and cold gas efficiencies, gas

64 yields and HHV of the product gas as compared to single fuel gasification (Masnadi et al.,

65 2015c). The significant enhancement in the production of hydrogen during in-situ capture of

66 CO_2 by CaO sorbent has been observed (Masnadi et al., 2015a).

67 Different behaviours in the reactivity of chars produced from coal and biomass, both together

68 and separately (Ellis et al., 2015). Ellis et al. (2015) suggested that there is an interaction during

69 volatilisation that effects the reactivity and that is why specific and intrinsic rates were

70 observed to be lower when coal and biomass were pyrolyzed together. Potassium in biomass,

71 as excess potassium (K/Al >1), can result in enhanced coal gasification due to its catalytic

72 impact (Habibi et al., 2012). The catalytic impact of potassium in biomass when the biomass

73 to coal ratio reached 3:1, where the biomass supplied enough potassium to satisfy the minerals

74 in the coal ash to enhance coal gasification has been found in the literature (Masnadi et al.,

75 2015b).

76 Co-firing is a proven technology with a significant experience in Europe (Al-Mansour and

77 Zuwala, 2010). The share of biomass co-firing in conventional pulverised coal fired power

78 stations have increased by up to 20 % in the past decade with some installations demonstrating

79 a complete switch from coal to biomass (Cremers, 2009).

80 Biomass and coal have different burnout rates and therefore may be fed to the combustor at

81 different locations (Jia et al., 2016). Also, coal and biomass can be mixed before combustion

82 to achieve a better control of the combustion process (Sahu et al., 2014). In the co-firing

83 process, biomass is mixed with coal to achieve over 35 % volatile matter for a stable flame

84 (Biagini et al., 2002; Wang et al., 2009). In the UK, co-firing biomass with coal offers a better

85 opportunity as compared to a dedicated biomass plant due to relatively small bioenergy

86 resources (Gough and Upham, 2011). In addition, biomass power is produced in either old coal

87 power plants converted to operate on imported biomass, e.g. Drax 2 and Ironbridge 1 and 2

88 (Verhoest and Ryckmans, June 2014), or purpose built biomass power plants, e.g. Stevens

89 Croft (40MW) that uses sawmill waste (AG., 2014).

90 In modern coal fired power plants, biomass can be co-fired up to 15 % without steam boiler

91 modifications and existing environmental control systems can be used at higher biomass co-

92 firing rates with minor modification (IEA, January 2007). Moreover, co-firing gives

93 substantially higher net efficiency than that a dedicated biomass fired power plant can deliver

94 (Hetland et al., 2016). This makes co-firing a much less expensive option than building a

95   dedicated biomass power plant (IEA, January 2007). In the absence of financial incentives for

96   negative emissions and avoided carbon, co-firing can play a transitional role to minimise the

97   emission penalties in a cost effective way (ETI, 2016). Moreover, the plant can be adjusted to

98   perform optimally using different types of biomass (Hetland et al., 2016). If the biomass supply

99   is ceased, due to a short age of supply, natural calamities or logistic issues, coal is still available

100   to keep the lights on and life moving. Biomass combustion can generate various types of

101   pollutants depending upon the type of combustion technology employed, properties of the

102   biomass used and pollutant control measures adopted can be found in the literature (Loo and

103   Koppejan, 2002). Also co-firing contributes to the reduction in emissions of obnoxious gases,

104   such as SO_x and NO_x.

105   Immediate step changes in emissions reduction is required to control CO_2 concentration in the

106   atmosphere. If drastic measures are not adapted, then by the end of the century CO_2

107   concentration in the atmosphere could reach 650 ppmv, or even higher (Anderson and Bows,

108   2008). Reduction in GHG emissions can improve air quality (Driscoll et al., 2015; Thompson

109   et al., 2014; West et al., 2013) and also limit global warming. There are many GHG emissions

110   reduction options, such as energy savings and renewable energy technologies, but CCS,

111   amongst others, is considered to be a key technology to meet stringent climate targets

112   (Koornneef et al., 2012). CCS comprises three steps; capture from the point source, transport

113   and storage. Although the individual technologies have been demonstrated with much

114   operational experience and are relatively well understood, however, the deployment of a large

115   scale fully integrated commercial CCS process is a key challenge (Gough and Upham, 2011).

116   Most of the biomass power plants deployed are fairly small units (1-100MW$_e$) and this is due

117   to the limited local feedstock availability and high transportation costs (IEA, January 2007).

118   Due to this reason, costs associated with bioenergy with Carbon Capture and Storage (BECCS)

119   are likely to be higher as compared to those associated with fossil fuel fired power plants with

120 CCS (Azar et al., 2006). However, in the UK the Drax power plant has 4 GW total capacity

121 with 70 % biomass share, and it is big enough to deliver economies on a scale for capturing

122 CO_2 (ETI, 2016). Moreover, there is sufficient potential for bioenergy to make a significant

123 contribution to the global energy supply (Dornburg et al., 2010).

124 In order to meet the target of limiting the global warming to below 2 °C, more than 1 Gt/year

125 of negative emissions are required (Gasser et al., 2015) and BECCS significantly enhances the

126 chances of meeting these ambitious climate mitigation targets (Azar et al., 2010). Each unit of

127 energy produced from BECCS is twice as effective in mitigating emissions as the ones without

128 CCS (Muratori et al., 2016). BECCS may be referred to as the process of capturing CO_2

129 emissions from biomass fired power plants and storing CO_2 in geological formations, or using

130 as a feedstock to produce algal biomass which is then converted to transport fuel, animal feed

131 or plastics (Gough and Upham, 2011). BECCS can be used to produce electricity, heat, gaseous

132 and liquid fuels and result in net removal of CO_2 from the atmosphere, also termed as "negative

133 emission" (ETI, 2016). BECCS potentially could have 33 % share of overall emissions

134 mitigation by the end of the century (Klein et al., 2011). According to the Fifth Assessment

135 Report of the Intergovernmental Panel on Climate Change (IPCC) it will not be possible to

136 achieve the target of limiting global warming without the wide spread deployment of Bio-

137 Energy, CCS and their combination (IPCC, 2014). BECCS can reduce the cost of achieving

138 the climate target by offsetting CO_2 from other sectors such as transportation, which are more

139 expensive to decarbonise (Luckow et al., 2010).

140 BEECS is a natural technology to progress first as it is competitive with other clean

141 technologies, adds flexibility to the system, has capacity to deliver negative emissions and

142 reduces the overall cost of decarbonisation (Oxburgh, 2016). According to a recent report

143 published by the Energy Technologies Institute (ETI), about half of the UK's 2050 emissions

144 reduction target (c.55 million tonnes of negative annual emissions) could be delivered by

145   deploying BECCS and could reduce the cost of meeting GHG emissions targets of the UK by

146   up to 1 % of GDP and that BECCS is one of the few practical, scalable and economic

147   technologies having UK relevance for removing CO_2 from the atmosphere in large quantities

148   (ETI, 2016).

149   The most significant barrier to the deployment of BECCS is not technical but economic and

150   regulatory (Bhave et al., 2014). In the near future, cost saving will not be delivered through

151   fundamental technology break-through but through reducing costs by deployment (ETI, 2016).

152   According to the Global CCS Institute database, no BECCS demonstration project has, as yet,

153   materialised (GCCSI, 2016). There are some bioethanol production based on BECCS projects

154   currently in operation (GCCSI, 2011) but power based BECCS projects are almost non-

155   existent. The Mikawa biomass power plant (49 MW) with CO_2 capture in Japan is aimed at

156   being operational in 2020 and it will be the first power plant in the world that is capable of

157   delivering negative emissions (Toshiba, 2016). The Maasvlakte power plant 3 (MPP3) in the

158   Netherlands has a capacity of 1070 MW_e and it became operational in 2015 being capable of

159   accepting up to 30 % biomass and is CCS ready subject to commercial decision (GCCSI, 2015).

160   According to a recent report by the Global CCS Institute (GCCSI, 2016), the Illinois Industrial

161   CCS project (1 Mtpa CO_2 capture capacity) is the world's first large scale industrial BECCS

162   project and is expected to begin operation in early 2017. The technology will move closer to

163   commercialisation as more demonstration projects come online (Gough and Upham, 2011).

164   In spite of all the benefits of BECCS, the deployment of CCS may be delayed due to the

165   temptation that BECCS can remove the CO_2 already emitted to the atmosphere (Muratori et

166   al., 2016) and thus can be deployed at a later date. However, this notion of delaying will lead

167   to catastrophic consequences to the world in terms of environmental as well as economic

168   implications.

1.1 Novelty and Contribution

Process modelling is used as an effective mean for better understanding for different operating levels of the power plant with CO_2 capture due to lower cost in comparison to pilot-scale and demonstration studies. The base load performance of the power plant for fossil fuels is successfully investigated through process modelling and simulation. The reporting of part-load analysis of the power plant for fossil fuels with CO_2 capture is limited and few studies can be found in the literature (Adams and Mac Dowell, 2016; Alobaid et al., 2014; Biliyok et al., 2012; Fernandez et al., 2016; Hanak et al., 2015; Jordal et al., 2012; Möller et al., 2007; Nord et al., 2009). However, most of the studies report the part-load performance and operational flexibility of a standalone natural gas power plant (Alobaid et al., 2014) or their integration with the amine-based CO_2 capture plant for interim operation and/or by-pass of the CO_2 capture plant (Adams and Mac Dowell, 2016; Jordal et al., 2012; Möller et al., 2007; Nord et al., 2009). The part-load operation of the coal-fired power plant integrated with an amine-based CO_2 capture plant has been reported in the literature (Fernandez et al., 2016; Hanak et al., 2015). Fernandez et al. (2016) have discussed the operational flexibility of the coal-fired power plant, with interim solvent regeneration and CO_2 capture plant by-pass at peak-load demand, however, it lacks the comprehensive details of the process and its parameters. Hanak et al. (2015) have reported the thorough details of the whole process of the coal-fired power plant integrated with CO_2 capture plant, at base-load and part-load performance. However, none have taken the biomass into consideration either at base-load or at part-load operation, neither as direct-firing nor as co-firing of coal with biomass.

The above discussion has shown that BECCS is a key technology to meet GHG emissions reduction targets and that co-firing biomass in coal fired systems has several advantages over dedicated biomass firing systems. Only a few studies have investigated BECCS for the commercial-scale application, as reported in the literature (Ali et al., 2017; Berstad et al., 2011;

194 Hetland et al., 2016). Berstad et al. (2011) have compared the three different power plants

195 integrated with MEA-based CO_2 capture plant including, natural gas, coal and biomass at

196 varying stripper pressure. Berstad et al. (2011) have found that the coal and biomass power

197 plants with a MEA-based CO_2 capture plant results in lower specific losses per unit of the CO_2

198 captured. However, this study was limited to the assessment of the base-load performance of

199 varying nominal power output for natural gas, coal and biomass -fired power plants with

200 limited details. Hetland et al. (2016) presented direct-firing and co-firing cases of coal and

201 biomass, however, only one case of co-firing is presented in detail with no attempt for the part-

202 load operation. Furthermore, the detailed information and parameters about the power plant

203 and CCS is lacking. Ali et al. (2017) have assessed the comparative potential of natural gas,

204 coal and biomass for the supercritical power plant integrated with CO_2 capture plant and CO_2

205 compression system. However, it does not take into account the co-firing and part-load

206 operation.

207 Due to limited information found in the open literature, it is important to assess the performance

208 of the part-load performance of direct-firing and co-firing of coal and biomass, especially

209 integrated with a CO_2 capture plant and CO_2 compression unit. Neither the integration of direct-

210 firing and co-firing with a CO_2 capture plant and CO_2 compression unit at the base-load has

211 been extensively studied before nor the part-load performance of the integration of direct-firing

212 and co-firing with CO_2 capture plant and CO_2 compression unit. Therefore, this paper presents

213 a detailed investigation of the co-firing of coal and biomass for commercial-scale pulverised

214 supercritical power plants. Further, the integration of the post-combustion CO_2 capture plant

215 (CCP) and CO_2 compression unit (CCU) is also investigated. Two co-firing scenarios of coal

216 and biomass are investigated at base-load operation of the power plants, i.e. constant heat input

217 (CHI) and constant fuel input (CFF), and the details of which are described in the respective

218 sections. Furthermore, the part-load operation (80, 60 and 40 %) is analysed for co-firing of

219   coal and biomass and integrated with CCP and CCU. Therefore, the theme of the present study

220   is to analyse the base-load performance of the direct-fired and co-fired coal and biomass power

221   plants integrated with CCP and CCU for the CHI and CFF cases. Furthermore, extending the

222   scope of the study towards the part-load operation at different power ratings for both direct-

223   fired and co-fired coal and biomass power plants integrated with CCP and CCU for CFF case.

224   The whole investigation is realised by the process modelling and simulation tool, Aspen Plus.

225   The solvent employed is monoethanolamine (MEA) of 30 wt. % strength with 90 % of the CO_2

226   capture efficiency. This paper is structured as follows. In Section 2, the process description,

227   along with the modelling strategy, is described in detail. This is followed by the base-load and

228   part-load modelling framework. In Section 3, the results and discussions for the base-load and

229   part-load operation for the co-firing of coal and biomass is presented. Further, the effect of the

230   part-load on the operation of the CCP is also discussed. Finally, conclusions are drawn in

231   Section 4.

232

233
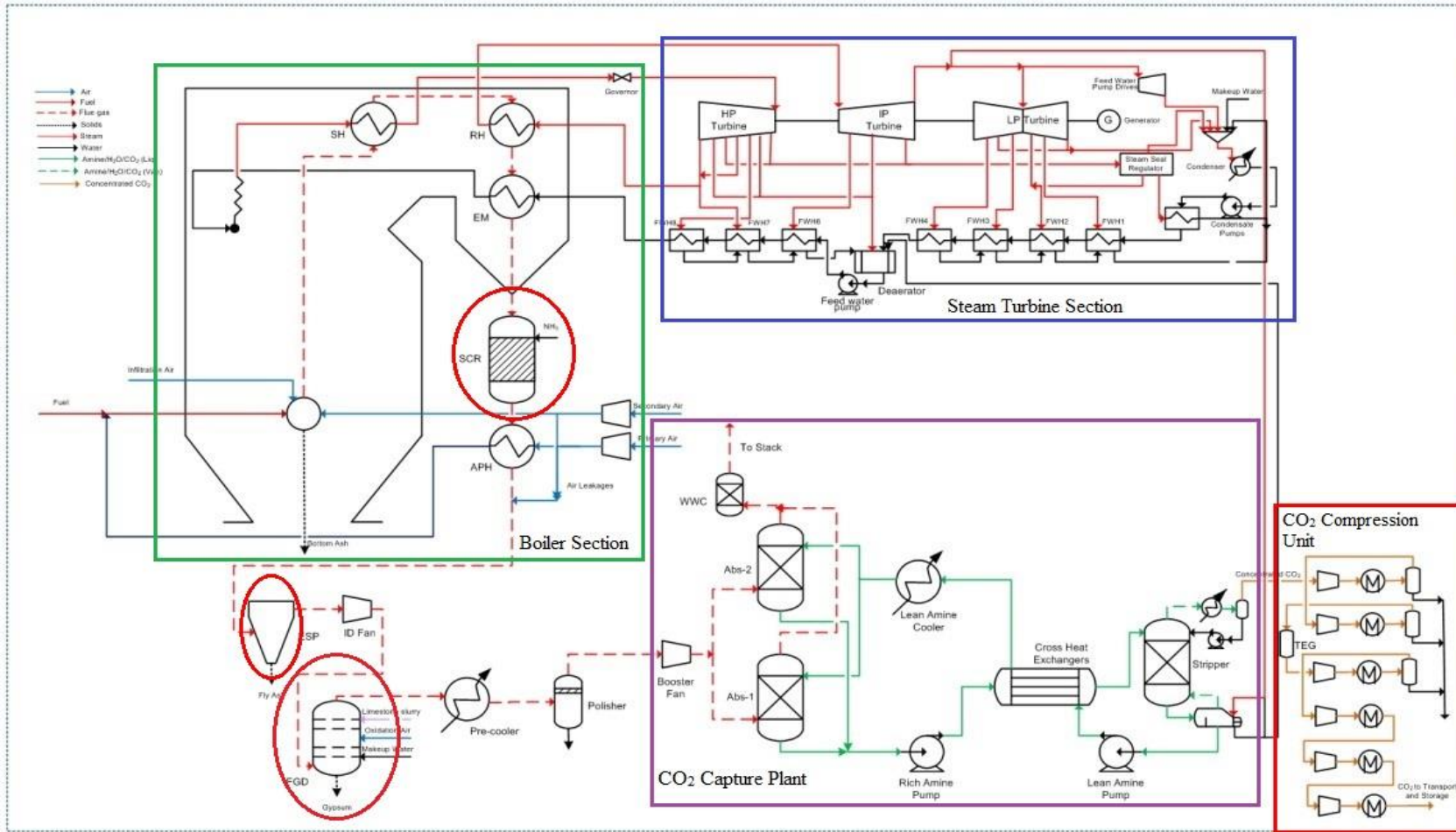
Figure 1 Process schematic of pulverised solid fuel power plant integrated with MEA-based CO_2 capture plant and CO_2 compression unit (Ali et al., 2017).

2. Process Description

The gross power output of the power plant is 800 MW_e based on the pulverised coal-fired supercritical power plant in the 2010 Report of the Department of Energy (Black, 2010). A schematic of the power plant model developed is shown in Figure 1. The steam generator for the supercritical-type boiler is once-through with superheater, reheater, economizer and air preheater. The steam specification for the supercritical steam turbine is 24.1/593/593 MPa/^{o}C/^{o}C with single reheat. Initially the feedwater is heated by bleeds of LP turbine, through four feedwater heaters, followed by the deaerator, and three feedwater heaters by bleeds of the HP turbine. The condenser operates at a saturation pressure of 7 kPa. Further, the power plant is equipped with flue gas treatment units, including the selective catalytic reduction unit for NO_x removal using ammonia and catalysts; fabric filters for the particulates removal; the flue gas desulphurization unit for the removal of the SO_2 using the wet limestone forced oxidation process; and the CO_2 capture plant for the removal of the CO_2 using MEA-based reactive absorption and desorption. More details of the flue gas treatment can be found in Ali et al. (2017).

The CO_2 capture plant (CCP) is based on post-combustion CO_2 capture technology using reactive absorption and desorption. The CO_2 capture plant consists of two absorbers and one stripper. The CO_2 released from the stripper is compressed to a final pressure of 153 bar using a six-stage CO_2 compression unit (CCU) equipped with intercoolers and knock-out drums. The tri ethylene glycol unit is used at the third stage to maintain the H_2O specification of the dense phase CO_2 stream.

 The air after the split is blown through primary and secondary fans, where the primary fan after air preheating is used to carry the fuel to the boiler, and the secondary air is fed at the latter stage of the boiler. Tertiary air and air leakages are also indicated in the boiler section

259   which is indicated by a green rectangle in Figure 1. The flue gas after combustion of the fuel,

260   either coal, biomass or co-firing of coal and biomass, is used for steam generation in the

261   superheater, reheater and economiser after which the flue gas is cleaned of the NO_x emissions

262   through the SCR as indicated by the red circle in the boiler section of Figure 1. The flue gas is

263   then used to preheat the incoming air from the primary blowers and then the flue gas is cleaned

264   from particulate matter in the ESP, before injecting it to the FGD for SO_2 removal which is

265   indicated by the red circles in Figure 1. After that the flue gas is either vented to the chimney

266   or sent to the CCP and CCU sections for the CO_2 removal and compression.

267   The boiler feed water after preheating through the feedwater heaters and treatment through the

268   feedwater deaerating is saturated in the economiser. The saturated steam is then superheated in

269   the superheater. The superheated steam from the superheater is sent to the HP turbine for power

270   generation, the steam after the HP turbine is passed through the reheater and is boosted and

271   passed through the IP turbine. The steam after the pressure reduction in the IP turbine is sent

272   to the LP turbine and a portion to the reboiler of the CCP section. The leakages from slip

273   streams in each section of the turbines are used to preheat the boiler feedwater in the steam

274   turbine section as shown by the blue rectangle in Figure 1.

275   The CCP section indicated by the purple rectangle in Figure 1 consists of two absorbers and

276   one stripper. The flue gas after the pressure increase in the blower is split into two parts for

277   each absorber. The flue gas after stripping the CO_2 from the flue gas using 30 wt. % MEA

278   solution is vented to the chimney. The rich solvent with higher concentration of the CO_2 is

279   pumped and heated through the cross-heat exchanger and then fed to the top of the stripper for

280   the regeneration of the solvent through the steam extracted from the IP-LP cross over section

281   of the steam turbine section. The solvent after regeneration is pumped, cooled and fed to the

282   top of the absorber. The CO_2 from the CCP is compressed through six stages of the compressors

283 with inter-stage coolers to reach the final pressure of 153 bar. The CCU section is shown by

284 the red rectangle in Figure 1.

285 The proximate and ultimate analysis of the coal and biomass is shown in Table 1. The coal

286 selected is from the 2010 Report of U.S. Department of Energy (Black, 2010), to have a fair

287 comparison and verification of the results. In spite of the interest in carbon capture and storage,

288 there is less freely available data in the open literature with complete information to rigorously

289 model and validate the supercritical coal-fired power plant except the data reported by Black

290 (2010). Therefore, the composition of coal is fixed to be the same as that found in (Black, 2010)

291 for a fair comparison. The biomass selected in Table 1 is the U.S. forestry residue pellets.

292 Further, the biomass is selected as it will be a basis for future research and experimentation by

293 the UK Carbon Capture and Research Centre's (UKCCSRC) at the Pilot-Scale Advanced CO_2

294 Capture Technology (PACT) National Core Facilities. The experimental data obtained at the

295 PACT facility will be used to validate the models and to perform further assessments. The

296 various case studies performed in this study are case-specific as varying the composition of the

297 coal and biomass are not assessed, however, the conclusions of this study are reasonably

298 general for different co-firing cases covering a wider range of fuel compositions.

299 Table 1 Proximate, ultimate and heating value of coal (Black, 2010) and biomass (Al-Qayim et al.,

300 2015).

	Coal		Biomass Pellets	
Proximate Analysis	As-received (wt. %)	Dry (wt. %)	As-received (wt. %)	Dry (wt. %)
Moisture	11.12	0.00	6.69	0.00
Volatile Matter	34.99	39.37	78.10	83.70
Ash	9.70	10.91	0.70	0.75

Fixed Carbon	44.19	49.72	14.51	15.55
Ultimate Analysis	As-received (wt. %)	Dry (wt. %)	As-received (wt. %)	Dry (wt. %)
C	63.75	71.72	48.44	51.87
S	2.51	2.82	<0.02	0.02
H	4.50	5.06	6.34	6.79
N	1.25	1.41	0.15	0.16
O	6.88	7.75	37.69	40.37
Ash	9.70	10.91	0.70	0.75
Cl	0.29	0.33	<0.01	0.01
HHV (kJ/kg)	27113	30506	19410	20802
LHV (kJ/kg)	26151	29444	18100	19398

301

2.1 Modelling Details

303 As mentioned in Section 1.1, the modelling and simulation of different cases of coal and

304 biomass and their part-load operation is realised in Aspen Plus. The base-case model of super-

305 critical coal-fired power plant is based on the previous work (Ali et al., 2017). The property

306 package employed for the thermodynamic estimation is Peng-Robinson with the Boston-

307 Mathias modification for the boiler, and IAPWS-95 for the steam cycle of the power plant.

308 The boiler efficiency of 88 % and excess air of 15 % were chosen as recommended in the

309 literature (Stultz and Kitto, 1992). The boiler chemistry is based on the minimization of Gibb's

310 free energy and is used as an equilibrium criterion. It is important to mention here that the non-

311 idealities of the coal and biomass combustion are not taken into consideration. Therefore, the

312 effect of heavy components and tar formation on the combustion kinetics and behaviour for

313 direct-fired and co-fired coal and biomass is outside the scope of the present research. The

314 boiler efficiency and turbine thermal input assists in the estimation of fuel flow rate which

315 further assists in the estimation of air flow rates. The flow rate requirement of ammonia for the

316 SCR unit is estimated from its principal reactions. Similarly, for the FGD unit, the flow rate

317 requirements for lime stone, make-up water and oxygen are estimated based on its principal

318 reactions. The principal reactions for the SCR and FGD units are presented in Table 2. The

319 boiler and steam turbine sections models are validated in the literature (Ali et al., 2017) and

320 verified by the 2010 Report of the Department of Energy (Black, 2010).

321   Table 2: Principal reactions involved in SCR, FGD and CCP.

Reactions	Reaction Number
Selective Catalytic Reduction Unit	
$4NO + 4NH_3 + O_2 \rightarrow 4N_2 + 6H_2O + heat$	(1)
$2NO_2 + 4NH_3 + O_2 \rightarrow 3N_2 + 6H_2O + heat$	(2)
Flue Gas Desulphurization Unit	
$CaCO_3(s) + SO_2(g) + 0.5H_2O \rightarrow CaSO_3 \cdot 0.5H_2O + CO_2(g)$	(3)
$CaCO_3(s) + SO_2(g) + 0.5O_2 + 2H_2O \rightarrow CaSO_4 \cdot 2H_2O + CO_2(g)$	(4)
CO$_2$ Capture Plant	
$H_2O + MEAH^+ \leftrightarrow MEA + H_3O^+$	(5)
$2H_2O \leftrightarrow H_3O^+ + OH^-$	(6)
$HCO_3^- + H_2O \leftrightarrow CO_3^{2-} + H_3O^+$	(7)
$CO_2 + OH^- \rightarrow HCO_3^-$	(8)
$HCO_3^- + \rightarrow CO_2 + OH^-$	(9)
$MEA + CO_2 + H_2O \rightarrow MEACOO^- + H_3O^+$	(10)
$MEACOO^- + H_3O^+ \rightarrow MEA + CO_2 + H_2O$	(11)

322

323 The CCP is modelled using rate-based electrolyte non-random two liquid (ENRTL)

324 thermodynamic packages by incorporating its principal reactions. The design data summary

325 for the CCP is given in Table 4. The aqueous MEA solution with 30 wt. % strength is employed

326 to capture 90 % of the incoming CO_2 with 0.2 solvent loading. The CCP model is validated

327 against extensive experimental data in the previous work (Ali et al., 2016). The principal

328 reactions included in the model are mentioned in Table 2. The CCU is modelled with the final

329 pressure of 153 bar. The thermodynamic property package employed for the CCU model is

330 Lee Keser Plocker.

331 **2.2 Base-Load Modelling Framework**

332 The reference base-load model for the coal is developed based on the 2010 Report of the

333 Department of Energy (Black, 2010) with a boiler efficiency of 88 %, which assists in the

334 estimation of the fuel flow for 15 % excess air supplied to the boiler. The infiltration air is 2 %

335 of the total air. The different assumptions applied for the modelling of the different sections of

336 the power plant can be found in the quality guidelines provided by the US Department of

337 Energy (Chou et al., 2012, 2014). After analysing the performance of the direct-fired coal-

338 based power plant integrated with CCP and CCU, the co-firing of coal and biomass is

339 performed. The ultimate and proximate analysis of the coal and biomass are shown in Table 1

340 and it is clear that the biomass will behave differently when fired in the commercial-scale

341 power plant due to the reduced heating value and higher O/C ratio compared to coal. The co-

342 firing of the coal and biomass is incorporated by mixing the biomass with coal, thus defining

343 the common fuel feed composition. The different case studies for the co-firing of coal and

344 biomass are listed in Table 3.

345 Table 3 Pulverised supercritical co-firing of coal and biomass cases classification* (Ali, 2017).

Cases	Coal/Biomass percentage in fuel feed stream
Coal	100/0
C8B2	80/20
C6B4	60/40
C4B6	40/60
C2B8	20/80
Biomass	0/100

346 *where 'C' represents coal and 'B' represents biomass.

347 Table 4 MEA-based CCP design and operating parameters (Agbonghae et al., 2014).

Parameter	Value

Absorber	
Number of Absorbers	2
Packing	Mellapak 250Y
Packing Height [m]	23.04
Diameter [m]	16.13
Stripper	
Number of Stripper	1
Packing	Mellapak 250Y
Packing Height [m]	25.62
Diameter [m]	14.61
Specific Reboiler Duty [MJ/kg CO_2]	3.69
Flue Gas Flowrate [kg/s]	821.26
MEA concentration [kg/kg]	0.3
Lean CO_2 loading [mol/mol]	0.2
Liquid/Gas Ratio [kg/kg]	2.93
Stripper pressure (Ledda et al.)	1.62

348

349   To understand the behaviour of the biomass, two case studies are investigated based on the fuel

350   flowrate. First, the constant heat case (CHI), in which the heat transfer from the boiler to the

351   steam side is kept constant by varying the fuel flowrate while the second one, constant fuel

352   flowrate (CFF) case in which the heat transfer from the boiler to the steam side is varied by

353   keeping the fuel flowrate constant. The base-load performance of the co-firing of coal and

354   biomass is developed for both the CHI and CFF cases integrated with CCP and CCU. A

355   standard MEA-based CCP model, which can service the commercial-scale power plant at 100

356   % load operation, is developed which can capture 90 % of the CO_2 from the flue gas using a

357   30 wt. % aqueous MEA solution with a lean loading of 0.2. The design and operating

358 parameters of the MEA-based CCP are given in Table 4. The efficiency estimation whether at

359 base-load modelling or part-load modelling is estimated on the basis of the higher heating

360 value. Furthermore, the model predictions of the direct-fired coal-based power plant are in very

361 good agreement with the published data as reported by the author (Ali et al., 2017), and hence

362 the results and findings of the present research may be used with confidence in a $\pm$ 10 % margin.

363 **2.3 Part-Load Modelling Framework**

364 After developing the base-load performance, the CFF case is evaluated for the part-load

365 performance assessment as it will not result in a major redesign of the boiler section of the

366 power plant. The coal-fired power plant is considered as the basis for each part-load

367 assessment, and then the fuel switch from coal to biomass and co-firing of coal and biomass

368 are evaluated at each part-load operation. The part-load performance of the co-firing of coal

369 and biomass in the power plant integrated with CCP and CCU is analysed in this study within

370 a 40 to 100 % envelope in intervals of 20 %. Hence, part-load performance is estimated at 40,

371 60, 80 % of the base-load (100 %) power of the power plant for each co-firing case of coal and

372 biomass. The methodology discussed by Hanak et al. (2015) is adopted for the boundary

373 condition estimation at the part-load operation. The widely-followed control of the boilers are;

374 the fixed pressure control for the boiler allowing steam throttling and the sliding pressure

375 control for the boiler in which steam pressure follows the turbine load and is dictated by the

376 boiler feed water pump. The sliding pressure control for the boiler is adopted as it results in

377 reduced power consumption (Fernandez et al., 2016; Hanak et al., 2015). The heat transfer

378 areas and temperature differences for the superheater, economiser reheater, and air preheater

379 are kept constant as estimated by the direct-fired coal-based power plant case at base-load

380 performance. Similarly, the heat transfer areas and temperature differences for the feedwater

381 heaters are also kept constant, as estimated from the coal-fired power plant case at base-load.

382 However, the pressure drop for the heat exchangers is estimated following the equation:

383 $\quad \Delta p = \dfrac{fV^2 L}{2g\rho d}$ $\hfill$ (1)

384 Further, the pressure drops, which are based on homogenous flow conditions (Green, 2008) at

385 the part-load performance, are updated using average velocity at base and part-load and

386 pressure drops at base load, using the following equation (Hanak et al., 2015):

387 $\quad \Delta p_{part} = \dfrac{\left(\dfrac{V_{in_{part}} + V_{out_{part}}}{2}\right)^2}{\left(\dfrac{V_{in_{base}} + V_{out_{base}}}{2}\right)^2} \Delta p_{base}$ $\hfill$ (2)

388 The sliding pressure control of the boiler requires the estimation of the steam flowrates and

389 pressure at different points of the steam turbine section along with the efficiencies for each

390 turbine section. The constant temperature is maintained at each part-load performance from the

391 40 to 100 % load range by controlling the steam generation rate by the design specification rate

392 (Hanak et al., 2015). The well-known equation, the Stadola Law of Cones (Cooke, 1983;

393 Salisbury, 1950), is widely used in power plants for the off-design steam specifications

394 estimation. The Stadola Law of Cones is used in an iterative manner for the fixed condenser

395 pressure, and it is given as follows:

396 $\quad \dfrac{m_{in}}{m_{in_{base}}} = \dfrac{\mu\, p_{in}}{\mu_{base} p_{in_{base}}} \sqrt{\dfrac{p_{in_{base}} v_{in_{base}}}{p_{in} v_{in}}} \sqrt{\dfrac{1 - \left(\dfrac{p_{out}}{p_{in}}\right)^{\frac{n+1}{n}}}{1 - \left(\dfrac{p_{out_{base}}}{p_{in_{base}}}\right)^{\frac{n+1}{n}}}}$ $\hfill$ (3)

397 The isentropic efficiency is updated based on the base-load isentropic efficiencies of the turbine

398 section. Knopf (2011) proposed the estimation of the isentropic efficiency based on the optimal

399 design with 50 % of the reaction blading (a = 0.7071), for a constant shaft speed at different

400 part-loads. Hence, the isentropic efficiency at the part-load can be estimated by the following

401 equation (Knopf, 2011; Salisbury, 1950):

402
$$\frac{\eta_{part}}{\eta_{base}} \cong 2 \frac{a}{\frac{V_{in_{base}}}{V_{in_{part}}}} \left[\left(a - \frac{a}{\frac{V_{in_{base}}}{V_{in_{part}}}} \right) + \sqrt{\left(a - \frac{a}{\frac{V_{in_{base}}}{V_{in_{part}}}} \right)^2 + 1 - a^2} \right] \qquad (4)$$

403 At each part-load operation from 40 to 100 %, the effect of the integration of the CCP and CCU

404 is also investigated. The CCP at the part-load performance of the power plant is kept to be the

405 same size as reported in Table 4, as it is common in engineering practice to employ oversize

406 units for better performance (Jordal et al., 2012). Therefore, the CO_2 capture rate is fixed at 90

407 % for part-load performance with 0.2 lean loading of the MEA 30 wt. % aqueous solution. At

408 reduced flowrates, the CCU operation may be effected due to the flowrates approaching surge

409 conditions. It is understood that anti surge control option is available for the CCU.

410 **3 Results and discussion**

411 **3.1 Base-Load Performance**

412 The reference coal-fired power plant integrated with CCP and CCU model is developed based

413 on information provided in Sections 2.1 to 2.3 and Ali et al. (2017). Further, co-firing of coal

414 and biomass for the CHI and CFF cases is evaluated for integration with CCP and CCU. The

415 key performance results for supercritical co-firing coal and biomass power plants integrated

416 with CCP and CCU for CHI case are reported in Table 5 for the base-load performance. The

417 important results for co-firing coal and biomass in the pulverised supercritical power plants

418 integrated with CCP and CCU for CFF case are reported in Table 6 for the base-load

419 performance. The process flow diagram of the base-load direct-firing coal case with process

420 parameters is indicated in Figure A-1.

421 Table 5 Important results for co-firing of coal and biomass in the pulverised supercritical power plants

422 integrated with CCP and CCU for CHI case at base-load performance.

Fuel type	Coal	C8B2	C6B4	C4B6	C2B8	Biomass

Fuel [kg/s]	71.3	75.6	80.4	85.9	92.3	99.6
Total air [kg/s]	729	726	723	720	712	702
Slag + Fly Ash [kg/s]	6.9	6	4.9	3.7	2.3	0.7
Main steam [kg/s]	630	630	630	630	630	630
Reheat from boiler [kg/s]	514	514	514	514	514	514
Steam to stripper [kg/s]	233	225	226	228	230	230
Flue gas, absorber inlet [kg/s]	832	830	829	827	819	804
CO_2 composition in flue gas [mol%]	13.28	13.42	13.56	13.73	13.93	14.35
Lean MEA solution, absorber inlet [kg/s]	2403	2414	2403	2453	2464	2470
Specific reboiler duty [MJ/kg CO_2]	3.686	3.679	3.677	3.675	3.674	3.673
Total compression duty [MW_e]	44.9	45.26	45.03	46.04	46.29	46.46
Fuel heat input, HHV [MW_{th}]	1933	1933	1933	1933	1933	1933
Power without steam extraction [MW_e]	800	800	800	800	800	800
Power with steam extraction [MW_e]	664	662	659	658	657	656
Power without CCP and CCU [MW_e]	758	758	758	758	758	758
Power with CCP only [MW_e]	602	600	598	597	596	596
Power with CCP and CCU [MW_e]	557	554	553	551	550	549
Efficiency without CCP and CCU [%]	39.22	39.3	39.3	39.3	39.3	39.3
Efficiency with CCP only [%]	31.16	31.02	30.94	30.86	30.83	30.82
Efficiency with CCP and CCU [%]	28.84	28.68	28.61	28.48	28.43	28.41

423   Table 6 Important results for co-firing of coal and biomass in the pulverised supercritical power plants

424   integrated with CCP and CCU for CFF case at base-load performance.

Fuel type	Coal	C8B2	C6B4	C4B6	C2B8	Biomass
Fuel [kg/s]	71.3	71.3	71.3	71.3	71.3	71.3
Total air [kg/s]	729	685	641	598	550	502
Slag + Fly Ash [kg/s]	6.9	5.6	4.4	3.1	1.8	0.5

Main steam [kg/s]	630	596	560	528	485	452
Reheat from boiler [kg/s]	514	486	457	431	396	369
Steam to stripper [kg/s]	233	212	198	188	176	163
Flue gas, absorber inlet [kg/s]	833	784	735	686	634	575
CO_2 composition in flue gas [mol%]	13.28	13.41	13.56	13.72	13.92	14.34
Lean MEA solution, absorber inlet [kg/s]	2403	2278	2128	2023	1889	1744
Specific reboiler duty [MJ/kg CO_2]	3.686	3.673	3.666	3.654	3.643	3.634
Total compression duty [MW_e]	44.9	42.8	40.06	38.22	35.82	33.21
Fuel heat input, HHV [MW_{th}]	1933	1823	1713	1603	1477	1384
Power without steam extraction [MW_e]	800	759	713	673	618	576
Power with steam extraction [MW_e]	664	627	590	555	509	475
Power without CCP and CCU [MW_e]	758	718	672	633	579	538
Power with CCP only [MW_e]	602	567	532	499	455	423
Power with CCP and CCU [MW_e]	557	524	492	461	419	390
Efficiency without CCP and CCU [%]	39.22	39.36	39.25	39.50	39.19	38.86
Efficiency with CCP only [%]	31.16	31.09	31.04	31.11	30.78	30.58
Efficiency with CCP and CCU [%]	28.84	28.75	28.70	28.72	28.36	28.18

425 The co-firing of coal and biomass results in more fuel feed requirement as the fraction of the

426 biomass in the fuel stream increases for the CHI case and resulted in 40 % higher fuel flowrate

427 for 100 % biomass in the fuel feed stream. However, the co-firing of coal and biomass causes

428 considerable derating as the fraction of the biomass in the fuel stream increases for the CFF

429 case and an overall 30 % derating of the power output capacity is expected for a complete

430 switch to biomass compared to the reference coal power plant either integrated with CCP and

431 CCU or not. The 44 and 49 % decrease in power output is expected when CCP and CCU,

432 respectively, is integrated with the biomass fired plant compared with a standalone coal power

433 plant.

434   However, the amount of the flue gas decreases and the CO_2 content in the flue gas increases,

435   for the increased fraction of the biomass in the fuel due to the higher O/C ratio in the biomass

436   for both the CHI and CFF cases. Also this results in higher specific CO_2 emissions from power

437   plants when the biomass share in the fuel feed stream increases; resulting in more specific CO_2

438   capture from the power plant (Ali, 2017).

439   It is worth noting that the CO_2 composition in the flue gas and other process parameters of the

440   direct-firing for the coal-fired and biomass-fired power plant are in good agreement with the

441   values found in the literature (Al-Qayim et al., 2015; Hetland et al., 2016). Further, the amine-

442   based CCP is extensively validated by the author in the literature (Akram et al., 2016; Ali et

443   al., 2016). However, the literature lacks the data for the comparison of the process parameters

444   with the reported values for the process validation and verification.

445   Moreover, if the biomass used is sustainably grown, it will result in more negative emissions

446   from the system. Thus, results in a lower flow rate of the flue gas with higher concentration of

447   the CO_2, hence lower solvent requirements for scrubbing, which decreases the specific reboiler

448   duty. The effect of co-firing coal and biomass on the CO_2 composition in the flue and specific

449   reboiler duty is given in Figure 2. However, there is a large decrease in specific reboiler duty

450   for the CFF cases as compared to the CHI cases and this is due to the lower flue gas flowrates

451   for the CFF cases and this results in the lower specific reboiler duty. The literature lacks

452   sufficient data to verify or validate the CFF and CHI cases investigated in this study. However,

453   the base cases of the coal-fired power plant was validated and verified by the author (Ali et al.,

454   2017) and therefore the results of the CFF and CHI cases may be considered to be reliable.

The boiler model assumes an equilibrium approach, where the oxygen-rich environment will promote complete combustion. However, it is known that direct biomass combustion or co-combustion produces undesired pollutants, such as tar aerosols (e.g. polycyclic aromatic hydrocarbons (PAH)), soot, fine char particles and alkali-based aerosols (Williams et al., 2012). Experimental studies have shown that biomass (corn stalk and pine sawdust) addition for co-combustion decreases PAHs formation compared to coal combustion; particularly, 3-ring PAHs and higher rings are decreased for the blend cases (Zhou et al., 2016). Therefore, it is expected that for the presented co-firing cases, tar formation will decrease compared to coal combustion.

Co-firing of coal and biomass have substantial effect on the emission control technologies integrated with the power plant. As the sulphur content in the biomass is low, as reported in Table 1, the amount of by-product gypsum produced decreases with the increased share of biomass in the fuel feed stream. Hence, the FGD unit may not be required in the co-firing of coal and biomass at the higher biomass shares and the polisher unit may be enough to meet the SO_2 requirements at the absorber inlet of the CCP. In addition, the slag and fly ash decrease substantially when coal is replaced by biomass for both the CHI and CFF cases. The detailed key performance results for the different cases of the co-firing of the coal and biomass can be found in Tables A.1 and A.2 in the Appendix A for the CHI and CFF, respectively, for the base-load operation for more interpretation and explanation.
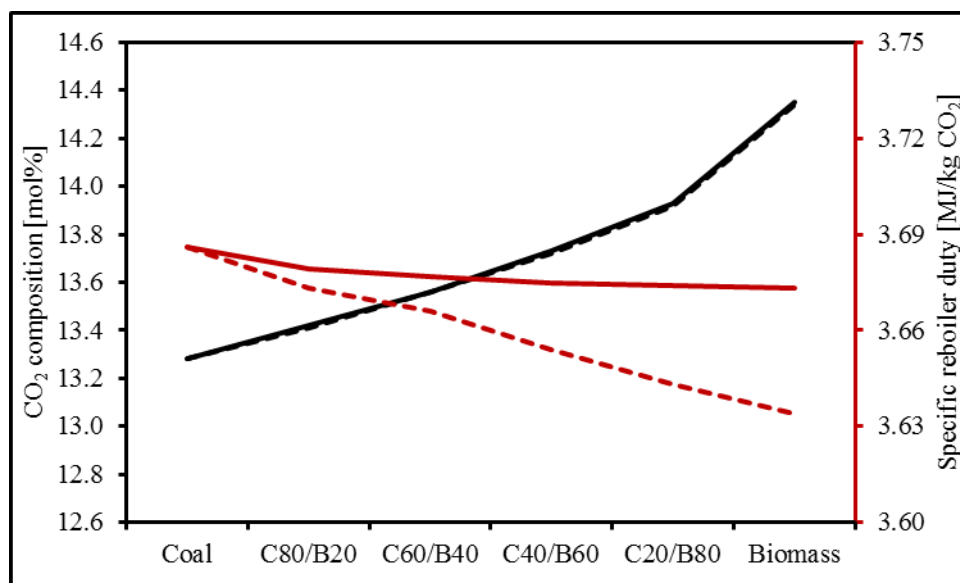
Figure 2 Impact of co-firing coal and biomass on the CO_2 composition in the flue gas and specific reboiler duty (where solid line represents CHI case and dashed line represents CFF case).

The net power output and net efficiency decreases when the share of biomass fraction in the fuel feed stream increases and this is due to a higher auxiliary load on the system for the CHI cases. It is observed that the efficiency penalty of the power plant with CO_2 capture and compression systems increases by approximately 4.8 % when coal is totally replaced by biomass in the CHI cases. However, there is a slight increase in specific CO_2 compression work per unit of the CO_2 captured and the specific losses per unit of the CO_2 captured due to increase in CO_2 concentration in the flue gas.

The efficiency penalty of the CFF cases is the same as that observed for the CHI cases since the base power output considered for comparison is the de-rated power output and not 800 MW_e. Due to the decreased flow rate of the flue gas, the amount of the CO_2 captured through scrubbing also decreases and hence results in a 30 % decrease in solvent requirement to scrub CO_2. Hence, this results in a considerable increase in the specific CO_2 compression work per unit of the CO_2 captured and specific losses per unit of the CO_2 captured for different CFF cases of co-firing of coal and biomass.

491   Table 7 Important results for co-firing of coal and biomass in the pulverised supercritical power plants

492   integrated with CCP and CCU for the CFF case at 80, 60 and 40 % part-load performance.

Fuel type	Coal	C8B2	C6B4	C4B6	C2B8	Biomass
80 % part-load operation						
Fuel heat input, HHV [MW$_{th}$]	1615	1523	1432	1340	1248	1156
Power without steam extraction [MW$_e$]	640	604	567	530	493	457
Power with steam extraction [MW$_e$]	523	488	452	423	393	365
Power without CCP and CCU [MW$_e$]	606	571	534	499	461	426
Power with CCP only [MW$_e$]	472	439	405	377	349	323
Power with CCP and CCU [MW$_e$]	435	403	371	345	319	295
Efficiency without CCP and CCU [%]	37.52	37.46	37.33	37.15	36.97	36.86
Efficiency with CCP only [%]	29.24	28.87	28.27	28.14	27.95	27.92
Efficiency with CCP and CCU [%]	26.91	26.47	25.90	25.76	25.55	25.52
60 % part-load operation						
Fuel heat input, HHV [MW$_{th}$]	1262	1190	1118	1046	975	903
Power without steam extraction [MW$_e$]	480	452	425	398	370	343
Power with steam extraction [MW$_e$]	388	364	343	320	298	276
Power without CCP and CCU [MW$_e$]	454	427	400	374	346	320
Power with CCP only [MW$_e$]	349	326	307	296	264	244
Power with CCP and CCU [MW$_e$]	320	298	280	260	241	222
Efficiency without CCP and CCU [%]	35.98	35.85	35.79	35.72	35.50	35.40
Efficiency with CCP only [%]	27.66	27.42	27.43	27.24	27.1	26.99
Efficiency with CCP and CCU [%]	25.34	25.08	25.06	24.85	24.71	24.59
40 % part-load operation						
Fuel heat input, HHV [MW$_{th}$]	882	832	781	731	681	631
Power without steam extraction [MW$_e$]	320	301	281	263	245	226
Power with steam extraction [MW$_e$]	268	252	235	220	204	189

Power without CCP and CCU [MW$_e$]	303	284	264	247	229	210
Power with CCP only [MW$_e$]	241	226	210	196	181	167
Power with CCP and CCU [MW$_e$]	221	207	192	179	165	152
Efficiency without CCP and CCU [%]	34.30	34.12	33.84	33.73	33.61	33.32
Efficiency with CCP only [%]	27.37	27.20	26.91	26.82	26.58	26.48
Efficiency with CCP and CCU [%]	25.04	24.86	24.54	24.43	24.18	24.07

493
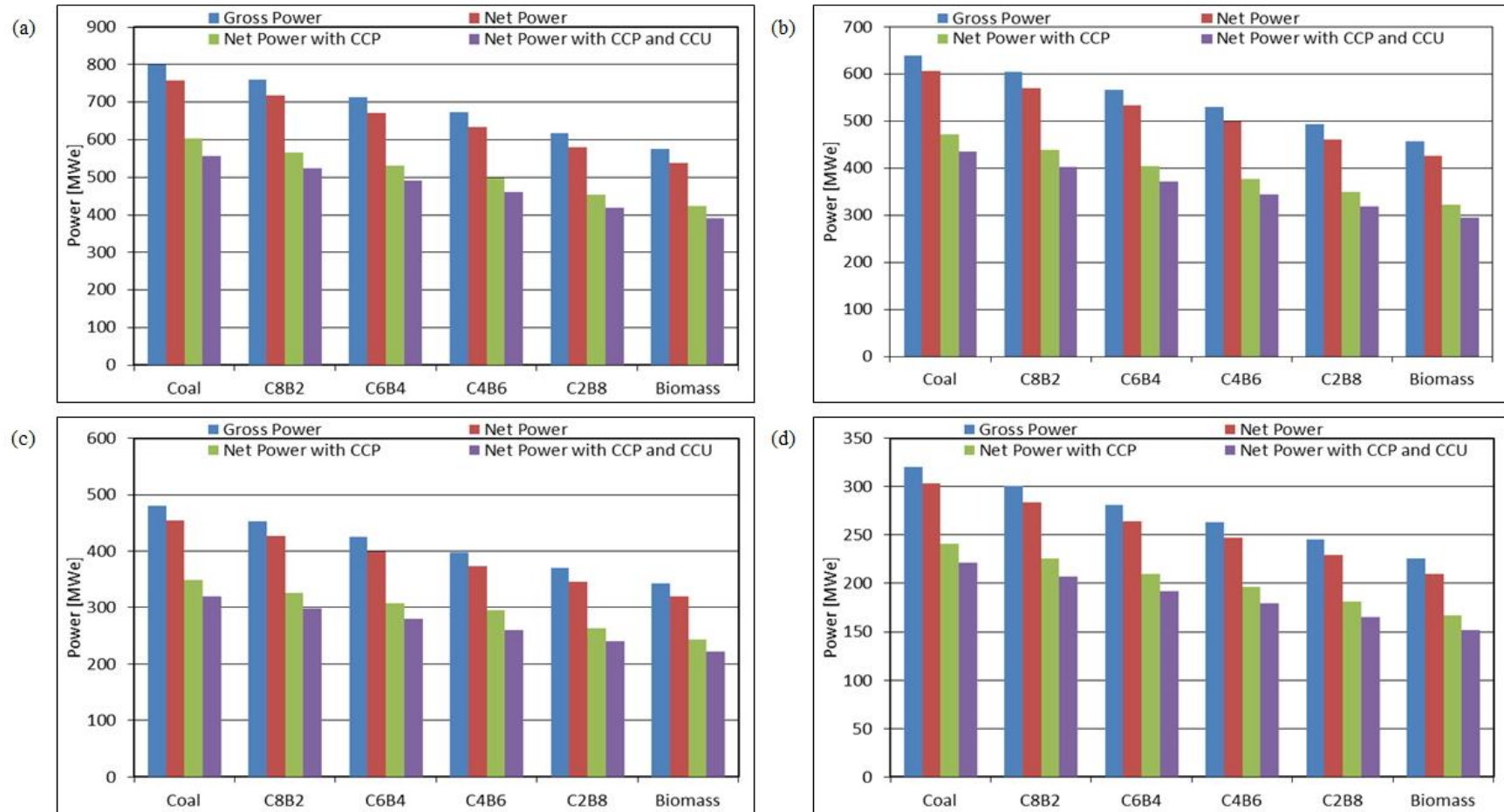
Figure 3 Power output from supercritical co-firing of coal and biomass power plants integrated with CCP and CCU for the CFF case at different part-load operations; (a) 100 % base-load operation; (b) 80 % part-load operation; (c) 60 % part-load operation; and (d) 40 % part-load operation.

498   **3.2 Part-Load Performance**

499   The part-load performance of the co-firing of coal and biomass integrated with CCP and CCU

500   from 40 to 100 % load is evaluated for the CFF case. The operating conditions for the part-load

501   operations were estimated based on the details provided in Section 2.3 for the referenced coal-

502   fired power plant and then the co-firing of coal and biomass is assessed for integration with

503   CCP and CCU for the CFF case for the part-load at 80, 60 and 40 % operation. Since, the case

504   evaluated is CFF, the fuel flowrate for each of the part-load operation is kept constant at the

505   same value as for the coal case at that part-load operation. Hence, this results in variable heat

506   input and variable power output from the power plant with and without integration with CCP

507   and CCU. However, co-firing of coal and biomass resulted in substantial power derating at

508   each part-load operation. The power derating for different part-load operation integrated with

509   CCP and CCU for the CFF case is shown in Figure 3 and listed in Table 7. The detailed

510   performance results for part-load operation at 80, 60 and 40 % are given in Tables A.3, A.4

511   and A.5, respectively. The derating in power output efficiency of the power plant not only

512   occurs horizontally when fuel is switched from coal to biomass at constant load operation, but

513   it also degrades perpendicularly downward when the load is shifted to the lower ones for the

514   same fuel type as listed in Table 3.

515   Furthermore, the behaviour of the power plant in terms of the power derating when fuel is

516   switched from coal to biomass at constant part-load operation is similar, as clearly observed in

517   Figure 3. An overall 30 to 32 % derating of the power output capacity is expected for complete

518   switch to biomass compared to the reference coal power plant at each of the part-load

519   operations either integrated with CCP and CCU or not. The 44 to 47 % and 49 to 51 % decrease

520   in power output is expected when CCP and CCU, respectively, is integrated with the biomass

521   fired plant compared with a standalone coal power plant at each part-load operation.

522 The specific reboiler duty behaviour is similar at each part-load operation as discussed in

523 Section 3.1 for the base-load operation. However, for a specific ratio of coal and biomass co-

524 firing, and subsequent part-load operation resulted in a decrease in specific reboiler duty,

525 although this decrease is not linear in nature. The finding of the decrease of non-linearity is in

526 line with the findings as found in the literature (Hanak et al., 2015). The decrease in specific

527 reboiler duty is 0.74 % for load change from 80 % to 60 % and is 1.05 % for the load change

528 from 60 % to 40 % of the part-load operation of the coal-fired power plant. Similarly, the

529 decrease in specific reboiler duty is 0.71 % for a load change from 80 % to 60 % and 1.13 %

530 for a load change from 60 % to 40 % of the part-load operation of the C8B2-fired power plant.

531 Similarly, the by-products gypsum from FGD, fly-ash from ESP, slag from boiler and NH_3

532 requirement in SCR decreases not only with part-load operation for the specific fuel feed, but

533 also for the co-firing at any of the part-load operation. It is important to mention here that an

534 extensive study for the part-load operation of the co-firing of coal and biomass has not been

535 found in the literature through which the results can be compared. However, since the base-

536 case model was extensively validated and verified, and the results obtained are comparable

537 then we have confidence in these results but this is a limitation of the present work.

538 As observed in the base-load operation, the flue gas treatment units may not be required when

539 the biomass share in the fuel increases. A similar observation is found for the part-load co-

540 firing of coal and biomass at different load operations. Process analysis revealed that the part-

541 load operation of coal-fired power plant resulted in only 28 % of the total power (800MW$_e$)

542 available on integration with CCP and CCU at 40 % load operation. The rest is degraded firstly

543 due to load change and secondly due to the parasitic load of the CCP and CCU. Similarly, at

544 part-load operation of the C8B2-fired power plant resulted in only 26 % of the total power

545 (800MW$_e$) available on integration with CCP and CCU at 40 % load operation and 24 % for

546 the C4B6 and eventually 19 % of the total power (800MW$_e$) available on integration with CCP

547   and CCU at 40 % load operation for the biomass-fired power plant. Figure 4 shows the decrease

548   in the power output due to the load change and further integration with CCP and CCU for

549   different co-firing of coal and biomass at various load changes in the form of percentage of the

550   total name plate power output of the power plant (800MW$_e$).
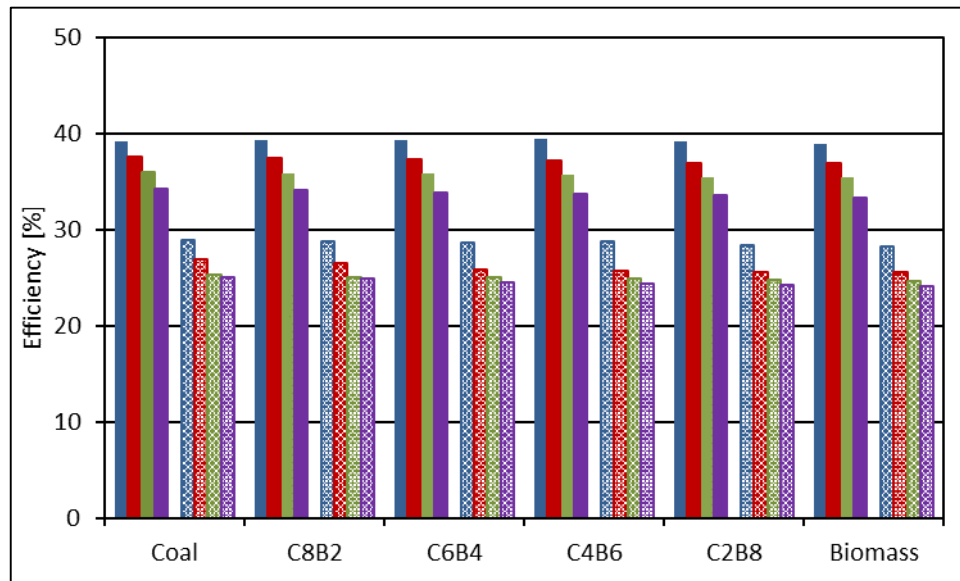
551
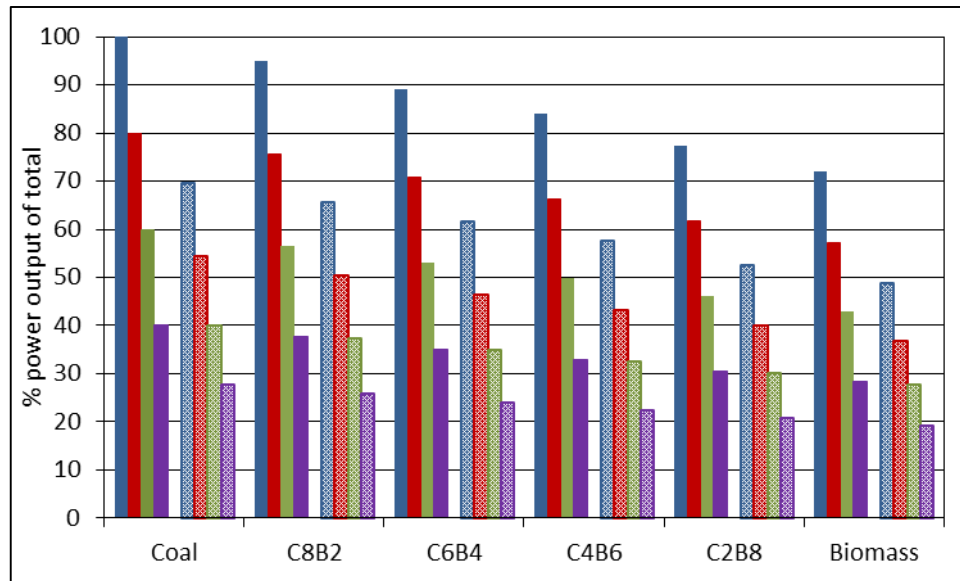
552

553   Figure 4 Percentage power output of the total name plate power output of the power plant (800MW$_e$)

554   for integration with CCP and CCU for CFF case at different part-load operation where solid coloured

555   bars are for % of the gross power output (of 800 MW$_e$) and hatched bars are for % of the net power

556   output (of 800 MW$_e$) when integrated with CCP and CCU. Where blue: 100 % base-load operation;

557   red: 80 % part-load operation; green: 60 % part-load operation; and purple: 40 % part-load operation.

558   The gross and net efficiency of direct-fired and co-fired coal and biomass power plants

559   integrated with CCP and CCU for different part-load operations is shown in Figure 5. It is

560   found that the gross efficiency and net efficiency of the power plants are reasonably constant

561   on the fuel switch from direct coal-firing to co-firing coal and biomass and to direct biomass-

562   firing. Since for the CFF case with co-firing the heat transfer decreases and hence the power

563   produced varies and hence the ratio of the power and HHV remains almost constant. However,

564 with the integration of the CCP and CCU there is a decrease in the efficiency as depicted as the

565 net efficiency in Figure 5.

566

567 Figure 5 Efficiency for integration with CCP and CCU for CFF case at different part-load operation

568 where solid coloured bars are for the gross efficiency and hatched bars are for the net efficiency when

569 integrated with CCP and CCU. Where blue: 100 % base-load operation; red: 80 % part-load operation;

570 green: 60 % part-load operation; and purple: 40 % part-load operation.

571

572 **3.3 Effect of Part-Load on Operation of CCP**

573 The net efficiency and power output of the power plant substantially reduces on integration

574 with CCP and CCU at the part-load operation in reference to the standalone base power plant,

575 and this will affect the operation and integration of the CCP (Hanak et al., 2015). Therefore,

576 the steam demand and extraction form the cross-over of the IP-LP turbine will vary during the

577 part-load operation. However, it is found that the power derating will not affect the operation

578 of the CCP as with the power derating, the demand of the steam for CO_2 stripping decreases.

579 Although, with power derating the IP-LP cross over pressure decreases and with a decrease in

580 steam pressure the stripping equilibrium will be disturbed due to the reduced steam pressure

581 and temperature (Fernandez et al., 2016). Furthermore, the amount of the CO_2 to be stripped

582   out of the reduced volume flue gas decreases and is proportional to the load decrease in the

583   power plant and results in less steam requirements (Fernandez et al., 2016). For example, at

584   40 % part-load operation, the steam temperature and pressure decreases to 254 $^{\circ}$C and 2.03 bar,

585   respectively for biomass-fired power plant integrated with CCP and CCU. The capture rate of

586   90 % is still achievable through modelling as the amount of CO_2 to be stripped also reduces

587   proportionally with the steam amount and the load changes.

588   However, it may not be possible to regenerate solvent at lower part-load operation when system

589   non-idealities may also be taken into consideration. For these scenarios, interim solvent

590   regeneration strategy may be adopted as suggested in the literature (Fernandez et al., 2016).

591   Therefore, a more robust model of the CCP or dynamic studies needs to be performed for the

592   evaluation of the CCP at part-load operation and this should be the subject for future research

593   work.

594   **4   Conclusions**

595   This paper has investigated the part-load performance of a power plant for co-firing of coal and

596   biomass in a commercial-scale pulverised supercritical power plant, integrated with an amine-

597   based post-combustion CO_2 capture plant (CCP) and CO_2 compression unit (CCU). It is

598   important to note that the results presented in this paper are for a specific composition of coal

599   and biomass. However, these results can be generalised to other compositions as different co-

600   firing scenarios are considered, and the predicted trends when increasing the biomass share

601   will still be valid. However, the results and conclusions are case specific and depend on the

602   composition of the coal and biomass selected. Furthermore, the model predictions of the direct-

603   fired coal-based power plant are in very good agreement with the published data as reported

604   by the author (Ali et al., 2017), and hence the results and findings of the present research may

605   be used with confidence with a ± 10 % margin. Two co-firing scenarios of coal and biomass

606   were investigated at base-load operation, and the following was concluded:

607   •   At constant heat input (CHI), more fuel is required as the percentage of biomass is

608   increased; e.g. for firing 100 % biomass, 40 % more fuel is fed than for 100 % coal.

609   •   At constant fuel input (CFF), derating occurs as the fraction of the biomass in the fuel

610   stream increases, e.g. 30 % derating of the power output capacity at firing 100 %

611   biomass compared to 100 % coal.

612   •   Higher specific CO_2 capture from the power plant is observed from when the share of

613   biomass in the fuel feed increases due to increases in the CO_2 content in the flue gas,

614   for both the CHI and CFF cases; it will result in negative emissions if sustainably-

615   grown biomass is used.

616   •   A larger decrease in specific reboiler duty is observed for the CFF cases as compared

617   to the CHI cases and this is due to the lower flue gas flowrates.

618   •   A FGD unit may not be required at the higher biomass shares, and a polisher unit may

619   be enough to meet the SO_2 requirements at the absorber inlet due to the low sulphur

620   content in biomass.

621   •   The net power output and net efficiency decrease when the fraction of biomass

622   increases for both cases. An efficiency penalty for integration with CO_2 capture and

623   compression systems increases by approximately 4.8 % when firing 100 % biomass in

624   the CHI case.

625   For part-load operation (80, 60 and 40 %) using the CFF case, the following was found:

626 • As expected, the power output decreases due to the load change and further integration

627 with CCP and CCU for different levels of co-firing of coal and biomass. Co-firing of

628 coal and biomass resulted in substantial power derating at each part-load operation. An

629 overall 30 to 32 % derating of the power output capacity is expected for 100 % biomass.

630 • At each part-load operation, specific reboiler duty decreases when the biomass fraction

631 increases.

632 • The by-products –gypsum from FGD, fly-ash from ESP, slag from boiler and NH_3

633 requirement in SCR– decrease for the co-firing at any part-load operation.

634 Future work will include the extension of the present work by including the various coal and

635 biomass compositions in to consideration. Furthermore, comparing the cost and economics of

636 the different systems under consideration.

637 **Nomenclature**

638 **Abbreviations**

639 Abs   absorber

640 APH   air preheater

641 BECCS   bioenergy carbon capture and storage

642 CCP CO_2 capture plant

643 CCS   carbon capture and storage

644 CCU CO_2 compression unit

645 CFF   constant fuel flowrate

646 CHI   constant heat input

647 EM   economiser

648	ENRTL	electrolyte non-random two liquid
649	ESP	electro static precipitator
650	ETI	Energy Technology Institute
651	FGD	flue gas desulphurization
652	FWH	feedwater heater
653	GHG	greenhouse gases
654	HP	high pressure
655	IAPWS	International Association for the Properties of Water and Steam
656	ID	induced draft
657	IP	intermediate pressure
658	IPCC	Intergovernmental Panel on Climate Change
659	LP	low pressure
660	MEA	monoethanolamine
661	MPP3	Maasvlakte power plant 3
662	PAH	polycyclic aromatic hydrocarbons
663	RH	reheater
664	SCR	selective catalytic reduction
665	SH	superheater
666	TEG	tri ethylene glycol
667	WWC	water wash column

668 **Parameters**

669 d   diameter (m)

670 f   friction factor

671 g $9.8 \ \mathrm{m/s}^2$

672 L   length of section (m)

673 m   mass flowrate (kg/s)

674 p   pressure (bar)

675 V   velocity (m/s)

676 v   specific volume (m^3/kg)

677 η   efficiency (%)

678 μ   kinematic viscosity (m^2/s)

679 ρ   density ($\mathrm{kg/m}^3$)

680 **Subscripts**

681 base   at base-load condition

682 in   input

683 part   at part-load condition

684 out   output

Acknowledgements

References

Adams, T., Mac Dowell, N., 2016. Off-design point modelling of a 420MW CCGT power plant integrated with an amine-based post-combustion CO_2 capture and compression process. Applied Energy 178, 681-702.

AG., S., 2014. Industrial Power: turbines for Biomass Plants – Products for Biomass-fired Power Generation and District Heating & Cooling Applications. Siemens AG., Energy Sector.

Agbonghae, E.O., Hughes, K.J., Ingham, D.B., Ma, L., Pourkashanian, M., 2014. Optimal Process Design of Commercial-Scale Amine-Based CO_2 Capture Plants. Industrial & Engineering Chemistry Research 53, 14815-14829.

Akram, M., Ali, U., Best, T., Blakey, S., Finney, K., Pourkashanian, M., 2016. Performance evaluation of PACT Pilot-plant for CO_2 capture from gas turbines with Exhaust Gas Recycle. International Journal of Greenhouse Gas Control 47, 137-150.

Al-Mansour, F., Zuwala, J., 2010. An evaluation of biomass co-firing in Europe. Biomass and Bioenergy 34, 620-629.

Al-Qayim, K., Nimmo, W., Pourkashanian, M., 2015. Comparative techno-economic assessment of biomass and coal with CCS technologies in a pulverized combustion power plant in the United Kingdom. International Journal of Greenhouse Gas Control 43, 82-92.

Ali, U., 2017. Process Simulation of Power Generation Systems with CO_2 Capture. PhD Thesis, University of Sheffield, Sheffield.

Ali, U., Agbonghae, E.O., Hughes, K.J., Ingham, D.B., Ma, L., Pourkashanian, M., 2016. Techno-Economic Process Design of a Commercial-Scale Amine-Based CO_2 Capture System for Natural Gas Combined Cycle Power Plant with Exhaust Gas Recirculation. Applied Thermal Engineering.

Ali, U., Font-Palma, C., Akram, M., Agbonghae, E.O., Ingham, D.B., Pourkashanian, M., 2017. Comparative potential of natural gas, coal and biomass fired power plant with post-combustion CO_2 capture and compression. International Journal of Greenhouse Gas Control 63, 184-193.

Alobaid, F., Karner, K., Belz, J., Epple, B., Kim, H.-G., 2014. Numerical and experimental study of a heat recovery steam generator during start-up procedure. Energy 64, 1057-1070.

Anderson, K., Bows, A., 2008. Reframing the climate change challenge in the light of post-2000 emission trends. Philosophical Transactions of the Royal Society 366, 3863-3883.

Azar, C., Lindgren, K., Mollersten, K., 2006. Carbon capture and storage from fossil fuels and biomass - costs and potential role in stabilizing the atmosphere. Climate Change 74, 47-49.

Azar, C., Lindgren, K., Obersteiner, M., Riahi, K., van Vuuren, D.P., den Elzen, K.M.G., Mollersten, K., Larson, E.D., 2010. The feasibility of low CO_2 concentration targets and the role of bioenergy with carbon capture and storage (BECCS). Climate change 100, 195-202.

Barbu, A., Dejean , F., Tomescu, M., Bottcher, H., Cludius, J., al., e., 2015, 4/2015. Trends and Projections in Europe 2015: Tracking Progress towards Europe's Climate and Energy Targets. European Environment Agency, Luxembourg.

Barbu, A., Schumacher, K., S, H., Hermann, H., Seimons, A., Zell, C., al., e., 2014, 6/2014. Trends and Projections in Europe 2014: Tracking Progress towards Europe's Climate and Energy Targets for 2020. European Environment Agency, Luxembourg.

BEIS, 2016. Renewable Heat Incentive (RHI) deployment data. Department for Business, Energy & Industrial Strategy.

Berstad, D., Arasto, A., Jordal, K., Haugen, G., 2011. Parametric study and benchmarking of NGCC, coal and biomass power cycles integrated with MEA-based post-combustion CO_2 capture. Energy Procedia 4, 1737-1744.

Bertrand, V., Dequiedt, B., Cadre, E.L., 2014. Biomass for electricity in the EU-27: Potential demand, CO_2 abatements and break even prices for co-firing. Energy Policy 73, 631-644.

Bhave, A., Taylor, R.S.H., Fennell, P., al., e., 2014. Screening and techno-economic assessment of biomass-based power generation with CCS technologies to meet 2050 CO_2 targets. Cambridge Centre for Computational Chemical Engineering, ISSN 1473-4273.

Biagini, E., Lippi, F., Petarca, L., Tognotti, L., 2002. Devolatilization rate of biomasses and coal biomass blends : an experimental investigation. Fuel 81, 1041-1050.

Biliyok, C., Lawal, A., Wang, M., Seibert, F., 2012. Dynamic modelling, validation and analysis of post-combustion chemical absorption CO_2 capture plant. International Journal of Greenhouse Gas Control 9, 428-445.

Black, J., 2010. Cost and performance baseline for fossil energy plants volume 1: bituminous coal and natural gas to electricity. Final report (2nd ed.) National Energy Technology Laboratory (2010 Nov) Report no.: DOE20101397.

Chou, V., Keairns, D., Turner, M., Woods, M., Zoelle, A., 2012. Quality guidelines for energy system studies: process modeling design parameters (National Energy Technology Laboratory) NETL. DOE-341/051314 pp 13–21.

Chou, V., Keairns, D., Turner, M., Woods, M., Zoelle, A., 2014. Quality guidelines for energy system studies: process modeling design parameters (National Energy Technology Laboratory) NETL. DOE-341/051314 pp 13–21.

EU Commission, 2006. Biomass Potential in Europe. European Commission (EC), Brussels, Belgium.

Cooke, D.H., 1983. Modeling of off-design multistage turbine pressures by Stodola's ellipse, Energy Incorporated PEPSE User's Group Meeting, Richmond, VA, Nov, pp. 2-3.

Cremers, M.F.G., 2009. Deliverable 4. Technical status of Biomass Co-Firing, 32. IEA Bioenergy Task Group.

Davidsson, K., Åmand, L.-E., Steenari, B.-M., Elled, A.-L., Eskilsson, D., Leckner, B., 2008. Countermeasures against alkali-related problems during combustion of biomass in a circulating fluidized bed boiler. Chemical Engineering Science 63, 5314-5329.

De, S., Assadi, M., 2009. Impact of cofiring biomass with coal in power plants–A techno-economic assessment. Biomass and Bioenergy 33, 283-293.

Dornburg, V., van Vuuren, D., van de Ven, G., Langeveld, H., Meeusen, M., Burger, N., al., e., 2010. Bioenergy revisited: Key factors in global potentials of bioenergy. Energy and Environmental Science 3, 258-267.

Driscoll, C.T., Buonocore, J.J., Levy, J.I., Lambert, K.F., Burtraw, D., Reid, S.B., Fakhraei, H., Schwartz, J., 2015. US power plant carbon standards and clean air and health co-benefits. Nature Climate Change 5, 535-540.

Ellis, N., Masnadi, M.S., Roberts, D.G., Kochanek, M.A., Ilyushechkin, A.Y., 2015. Mineral matter interactions during co-pyrolysis of coal and biomass and their impact on intrinsic char co-gasification reactivity. Chemical Engineering Journal 279, 402-408.

ETI, 2016. The evidence for deploying Bioenergy with CCS (BECCS) in the UK, An insights report from the Energy Technologies Institute. Energy Technologies Institute, Loughborough.

Fernandez, E.S., del Rio, M.S., Chalmers, H., Khakharia, P., Goetheer, E., Gibbins, J., Lucquiaud, M., 2016. Operational flexibility options in power plants with integrated post-combustion capture. International Journal of Greenhouse Gas Control 48, 275-289.

Gasser, T., Guivarch, C., Tachiiri, K., Jones, C., Ciais, P., 2015. Negative emissions physically needed to keep global warming below 2 °C. Nature Communications 6:7958, 1-7.

GCCSI, 2011. Global Status of BECCS Projects 2010. Global CCS Institute, Canberra, Australia.

GCCSI, 2015. Large Scale CCS Projects. the Global CCS Institute Database available on http://www.globalccsinstitute.com/projects/large-scale-ccs-projects. Assesed in January 2017.

781 GCCSI, 2016. The Global Status of CCS: 2016. Summary Report. Global CCS Institute, Canberra,
782 Australia.
783 Gough, C., Upham, P., 2011. Biomass energy with carbon capture and storage (BECCS or Bio-CCS).
784 Greenhouse Gases: Science and Technology 1, 324-334.
785 Green, D.W., 2008. Perry's chemical engineers' handbook, 8 ed. McGraw-hill New York.
786 Habibi, R., Kopyscinski, J., Masnadi, M.S., Lam, J., Grace, J.R., Mims, C.A., Hill, J.M., 2012. Co-
787 gasification of biomass and non-biomass feedstocks: synergistic and inhibition effects of switchgrass
788 mixed with sub-bituminous coal and fluid coke during CO_2 gasification. Energy & Fuels 27, 494-500.
789 Hanak, D.P., Biliyok, C., Manovic, V., 2015. Evaluation and modeling of part-load performance of coal-
790 fired power plant with postcombustion CO_2 capture. Energy & Fuels 29, 3833-3844.
791 Heller, M.C., Keoleian, G.A., Msnn, M.K., Volk, T.A., 2004. Life cycle energy and environmental benefits
792 of generating electricity from willow biomass. Renewable Energy 29, 1023-1042.
793 Hetland, J., Yowargana, P., Leduc, S., Kraxner, F., 2016. Carbon-negative emissions: Systemic impacts
794 of biomass conversion: A case study on CO_2 capture and storage options. International Journal of
795 Greenhouse Gas Control 49, 330-342.
796 Hughes, E.E., Tillman, D.A., 1998. Biomass cofiring: status and prospects 1996. Fuel processing
797 technology 54, 127-142.
798 IEA, January 2007. Energy Technology Essentials, ETE03. International Energy Agency, Paris, France.
799 IPCC, 2014. Climate Change 2014: Mitigation of Climate Change. Intergovernmental Panel on Climate
800 Change.
801 Jia, L., Geddis, P., Madrali, S., Preto, F., 2016. Determination of Emission Factors for Co-firing Biomass
802 and Coal in a Suspension Fired Research Furnace. Energy and Fuels 30, 7342-7356.
803 Jordal, K., Ystad, P.A.M., Anantharaman, R., Chikukwa, A., Bolland, O., 2012. Design-point and part-
804 load considerations for natural gas combined cycle plants with post combustion capture. International
805 Journal of Greenhouse Gas Control 11, 271-282.
806 Klein, D., Bauer, N., Bodirsky, B., Dietrich, J.P., Popp, A., 2011. Bio-IGCC with CCS as a long-term
807 mitigation option in a coupled energy-system and land-use model. Energy Proceedia 4, 2933-2940.
808 Knopf, F.C., 2011. Modeling, analysis and optimization of process and energy systems. John Wiley &
809 Sons.
810 Koornneef, J., van Breevoort, P., Hamelinck, C., Hendriks, C., Hoogwijk, M., Koop, K., Koper, M., Dixnob,
811 T., Camps, A., 2012. Global potential for biomass and carbon dioxide capture, transport and storage
812 up to 2050. International Journal of Greenhouse Gas Control 11, 117-132.
813 Ledda, C., Schievano, A., Scaglia, B., Rossoni, M., Acién Fernández, F.G., Adani, F., 2016. Integration of
814 microalgae production with anaerobic digestion of dairy cattle manure: an overall mass and energy
815 balance of the process. Journal of Cleaner Production 112, Part 1, 103-112.
816 Loo, S.V., Koppejan, J., 2002. Handbook of biomass combustion and co-firing. Twente University Press,
817 Enschede, the Netherlands.
818 Luckow, P., Wise, M.A., Dooley, J.J., Kim, S.H., 2010. Large-scale utilization of biomass energy and
819 carbon dioxide capture and storage in the transport and electricity sectors under stringent CO_2
820 concentration limit scenarios. International Journal of Greenhouse Gas Control 4, 865-877.
821 Mann, M., Spath, P., 2001. A life cycle assessment of biomass cofiring in a coal-fired power plant. Clean
822 Products and Processes 3, 81-91.
823 Masnadi, M.S., Grace, J.R., Bi, X.T., Ellis, N., Lim, C.J., Butler, J.W., 2015a. Biomass/coal steam co-
824 gasification integrated with in-situ CO_2 capture. Energy 83, 326-336.
825 Masnadi, M.S., Grace, J.R., Bi, X.T., Lim, C.J., Ellis, N., 2015b. From fossil fuels towards renewables:
826 Inhibitory and catalytic effects on carbon thermochemical conversion during co-gasification of
827 biomass with fossil fuels. Applied Energy 140, 196-209.
828 Masnadi, M.S., Grace, J.R., Bi, X.T., Lim, C.J., Ellis, N., Li, Y.H., Watkinson, A.P., 2015c. From coal towards
829 renewables: Catalytic/synergistic effects during steam co-gasification of switchgrass and coal in a
830 pilot-scale bubbling fluidized bed. Renewable Energy 83, 918-930.

831   Möller, B.F., Genrup, M., Assadi, M., 2007. On the off-design of a natural gas-fired combined cycle
832   with CO_2 capture. Energy 32, 353-359.

833   Muratori, M., Calvin, K., Wise, M., Kyle, P., Edmonds, J., 2016. Global economic consequences of
834   deploying bioenergy with carbon capture and storage (BECCS), Environmental Research Letters, pp. 1-
835   9.

836   NETBIOCOF, 2016. D14: First state-of-the-art report. Integrated European Network for Biomass Co-
837   firing (NETBIOCOF).

838   Nord, L.O., Anantharaman, R., Bolland, O., 2009. Design and off-design analyses of a pre-combustion
839   CO_2 capture process in a natural gas combined cycle power plant. International Journal of Greenhouse
840   Gas Control 3, 385-392.

841   Oladejo, J.M., Adegbite, S., Pang, C.H., Liu, H., Parvez, A.M., Wu, T., 2017. A novel index for the study
842   of synergistic effects during the co-processing of coal and biomass. Applied Energy 188, 215-225.

843   Ortiz, D.S., Curtright, A.E., Samaras, C., Litovitz, A., Burger, N., 2011. Near-Term Opportunities for
844   Integrating Biomass into the U.S. Electricity Supply. RAND Corporation.

845   Oxburgh, R., 2016. Lowest Cost Decarbonisation for the UK: The Critical Role of CCS. Report to the
846   Secretary of State for Business, Energy and Industrial Strategy from the Parliamentary Advisory Group
847   on Carbon Capture and Storage (CCS).

848   Rigamonti, L., Grosso, M., Biganzoli, L., 2012. Environmental assessment of refuse-derived fuel co-
849   combustion in a coal-fired power plant. Journal of Industrial Ecology 16, 748-760.

850   Sahu, S.G., Chakraborty, N., Sarkar, P., 2014. Coal–biomass co-combustion:Anoverview. Rnewable and
851   Sustainable Energy Reviews 39, 575-586.

852   Salisbury, J.K., 1950. Steam turbines and their cycles. Wiley.

853   Sebastián, F., Royo, J., Gómez, M., 2011. Cofiring versus biomass-fired power plants: GHG
854   (Greenhouse Gases) emissions savings comparison by means of LCA (Life Cycle Assessment)
855   methodology. Energy 36, 2029-2037.

856   Stultz, S., Kitto, J., 1992. Steam, Its Generation and Use, 1st Print. Babcock & Wilcox, AD.

857   Sung, Y., Lee, S., Kim, C., Jun, D., Moon, C., Choi, G., Kim, D., 2016. Synergistic effect of co-firing woody
858   biomass with coal on NOx reduction and burnout during air-staged combustion. Experimental Thermal
859   and Fluid Science 71, 114-125.

860   Thompson, T.M., Rausch, S., Saari, R.K., Selin, N.E., 2014. A systems approach to evaluating the air
861   quality co-benefits of US carbon policies. Nature Climate Change 4, 917-923.

862   Tilghman, M.B., Mitchell, R.E., 2015. Coal and biomass char reactivities in gasification and combustion
863   environments. Combustion and Flame 162, 3220-3235.

864   Tillman, D.A., 2000. Biomass cofiring: the technology, the experience, the combustion consequences.
865   Biomass and Bioenergy 19, 365-384.

866   Toshiba, 2016. Toshiba and Mizuho Information & Research Institute to Lead Japan's Largest CCS
867   Project. Press release available from: https://www.toshiba.co.jp/about/press/2016_07/pr2601.htm.
868   Assesed in January 2017.

869   Verhoest, C., Ryckmans, Y., June 2014. Industrial Wood Pellets: Report Pellcert. Laborelec.

870   Wang, C., Wang, F., Yang, Q., Liang, R., 2009. Thermogravimetric studies of the behaviour of wheat
871   straw with added coal during combustion. Biomass and Bioenergy 33, 50-56.

872   West , J., Smith, S.J., Silva, R.A., Naik, V., Zhang, Y., Adelman, Z., Fry, M.M., Anenberg, S., Horowitz,
873   L.W., Lamarque, J.F., 2013. Co-benefits of mitigating global greenhouse gas emissions for future air
874   quality and human health. Nature Climate Change 3, 885-889.

875   Williams, A., Jones, J., Ma, L., Pourkashanian, M., 2012. Pollutants from the combustion of solid
876   biomass fuels. Progress in Energy and Combustion Science 38, 113-137.

877   Zhou, C., Liu, G., Wang, X., Qi, C., 2016. Co-combustion of bituminous coal and biomass fuel blends:
878   Thermochemical characterization, potential utilization and environmental advantage. Bioresource
879   technology 218, 418-427.

880